AD-A087 293 STATE UNIV OF NEW YORK AT BUFFALO DEPT OF CHEMISTRY F/6 7/4
ELECTROCHEMICAL AND SPECTROSCOPIC STUDIES OF 9,10-ANTHRAQUINONE--ETC(U)
JUL 80 G T CHEEK, R A OSTERYOUNG N00014-79-C-0682
UNCLASSIFIED TR-2 NL

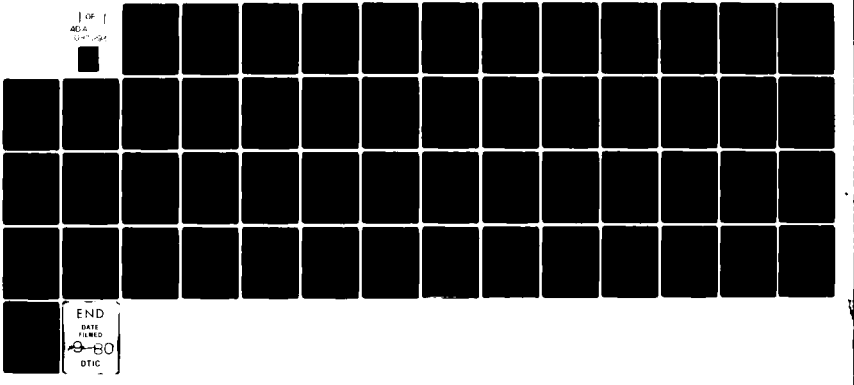

END
DATE FILMED
8-80
DTIC

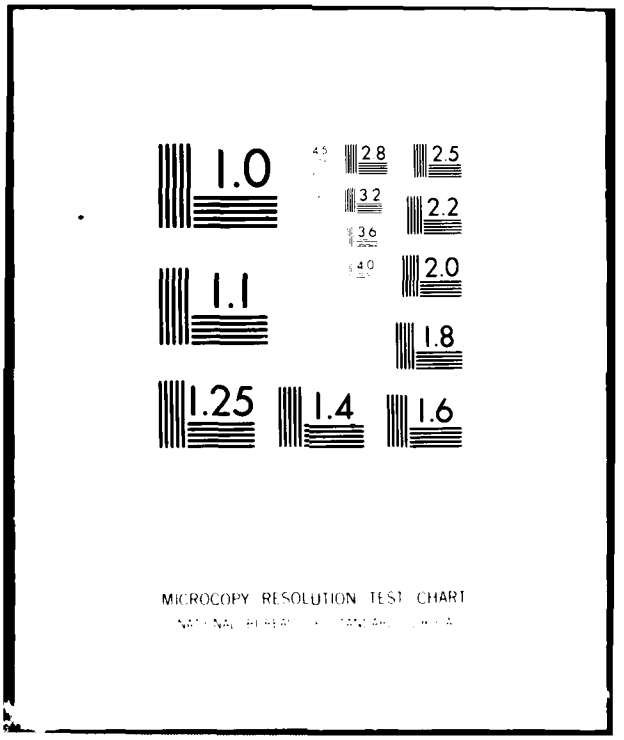
1.0
2.8
2.5
3.2
2.2
3.6
4.0
2.0
1.1
1.8
1.25
1.4
1.6
MICROCOPY RESOLUTION TEST CHART

LEVEL II

12

SECURITY CLASSIFICATION OF THIS PAGE (When Data Entered)

REPORT DOCUMENTATION PAGE	READ INSTRUCTIONS BEFORE COMPLETING FORM
1. REPORT NUMBER: Technical Report No. 2 — 2. GOVT ACCESSION NO.: AD-A087 293	3. RECIPIENT'S CATALOG NUMBER
4. TITLE (and Subtitle): Electrochemical and Spectroscopic Studies of 9,10-Anthraquinone in a Room-Temperature Molten Salt	5. TYPE OF REPORT & PERIOD COVERED: Technical report
	6. PERFORMING ORG. REPORT NUMBER
7. AUTHOR(s): Graham T. Cheek and R. A. Osteryoung	8. CONTRACT OR GRANT NUMBER(s): N00014-79-C-0682; F49620-79-C-0142
9. PERFORMING ORGANIZATION NAME AND ADDRESS: Department of Chemistry, State University of New York at Buffalo, Buffalo, New York 14214	10. PROGRAM ELEMENT, PROJECT, TASK AREA & WORK UNIT NUMBERS: NR TTR
11. CONTROLLING OFFICE NAME AND ADDRESS: Office of Navel Research/Chemistry Program, Arlington, VA 22217	12. REPORT DATE: July 1980; 13. NUMBER OF PAGES: 44
14. MONITORING AGENCY NAME & ADDRESS (if different from Controlling Office)	15. SECURITY CLASS. (of this report): Unclassified
	15a. DECLASSIFICATION/DOWNGRADING SCHEDULE

16. DISTRIBUTION STATEMENT (of this Report)

Approved for Public Release: Distribution Unlimited

DTIC ELECTE JUL 30 1980 S D E

17. DISTRIBUTION STATEMENT (of the abstract entered in Block 20, if different from Report)

18. SUPPLEMENTARY NOTES

Prepared for publication in Journal of the American Chemical Society

19. KEY WORDS (Continue on reverse side if necessary and identify by block number)

Chloroaluminate melts; infrared studies; room temperature molten salts; anthraquinone

20. ABSTRACT (Continue on reverse side if necessary and identify by block number)

The electrochemical and spectroscopic properties of 9,10-anthraquinone (AQ) in the low-temperature $AlCl_3$:n-butylpyridinium chloride (BuPyCl) molten salt system have been studied as a function of melt acidity. Infrared spectroscopic data indicate that AQ exists in the uncomplexed state in the basic melt (0.8 $AlCl_3$:1.0 BuPyCl). The electrochemical behavior in this region involves a single-process two-electron reduction (with slow electron transfer) of AQ to its dianion, the reduction mechanism probably proceeding

DD FORM 1 JAN 73 1473 EDITION OF 1 NOV 65 IS OBSOLETE

Unclassified

SECURITY CLASSIFICATION OF THIS PAGE (When Data Entered)

by an ECE pathway. Oxidation of the dianion back to AQ occurs at a potential considerably positive (600mV) of the potential for AQ reduction, thus indicating some interaction of the dianion with the melt. The complexation of AQ by $Al_2Cl_7^-$ in the acidic melt (1.2 $AlCl_3$:1.0 BuPyCl) produces AQ·2$AlCl_3$ as indicated both by infrared spectroscopy and chemical analysis. This complexation results in a shift in potential for the reduction process compared to the corresponding potential for AQ reduction in the basic melt of +1.4V. The reduction of AQ·2$AlCl_3$ also involves a single-wave two-electron process (with faster electron transfer than in the basic melt), thought to proceed by a disproportionation mechanism. Since the same separation in potentials for AQ·2$AlCl_3$ reduction and subsequent oxidation in the acidic melt was observed as that seen for AQ in the basic melt, some interaction of the dianion with the acidic melt is also evident. As the composition of the melt was varied through the neutral region (approx. 1.0 $AlCl_3$:1.0 BuPyCl), in which the acidity is changing rapidly, an additional process due to reduction of AQ·2$AlCl_3$ was observed; by adjustment of melt acidity by small additions of $AlCl_3$ or BuPyCl, a melt containing all three species AQ, AQ·$AlCl_3$, and AQ·2$AlCl_3$ could be obtained. Electrochemical studies of this system indicated that interconversion among the various species upon reduction is rather slow, an observation reflecting the low levels of $Al_2Cl_7^-$ present as well as the unbuffered nature of the melt in this region.

OFFICE OF NAVAL RESEARCH

Contract N00014-79-C-0682

TECHNICAL REPORT NO. 2

ELECTROCHEMICAL AND SPECTROSCOPIC STUDIES OF 9,10 ANTHRAQUINONE IN A ROOM TEMPERATURE MOLTEN SALT

by

GRAHAM T. CHEEK AND R. A. OSTERYOUNG

Prepared for Publication in

Journal of the American Chemical Society

Department of Chemistry
State University of New York at Buffalo
Buffalo, New York 14214

July, 1980

ABSTRACT

The electrochemical and spectroscopic properties of 9,10-anthraquinone (AQ) in the low-temperature $AlCl_3$:n-butylpyridinium chlorride (BuPyCl) molten salt system have been studied as a function of melt acidity. Infrared spectroscopic data indicate that AQ exists in the uncomplexed state in the basic melt (0.8 $AlCl_3$:1.0 BuPyCl). The electrochemical behavior in this region involves a single-process two-electron reduction (with slow electron transfer) of AQ to its dianion, the reduction mechanism probably proceeding by an ECE pathway. Oxidation of the dianion back to AQ occurs at a potential considerably positive (600mV) of the potential for AQ reduction, thus indicating some interaction of the dianion with the melt. The complexation of AQ by $Al_2Cl_7^-$ in the acidic melt (1.2 $AlCl_3$:1.0 BuPyCl) produces AQ·2$AlCl_3$ as indicated both by infrared spectroscopy and chemical analysis. This complexation results in a shift in potential for the reduction process compared to the corresponding potential for AQ reduction in the basic melt of +1.4V. The reduction of AQ·2$AlCl_3$ also involves a single-wave two-electron process (with faster electron transfer than in the basic melt), thought to proceed by a disproportionation mechanism. Since the same separation in potentials for AQ·2$AlCl_3$ reduction and subsequent oxidation in the acidic melt was observed as that seen for AQ in the basic melt, some interaction of the dianion with the acidic melt is also evident. As the composition of the melt was varied through the neutral region (approx. 1.0 $AlCl_3$: 1.0 BuPyCl), in which the acidity is changing rapidly, an additional process due to reduction of AQ·$AlCl_3$ was observed; by adjustment of melt acidity by small additions of $AlCl_3$ or BuPyCl, a melt containing

all three species AQ, $AQ \cdot AlCl_3$, and $AQ \cdot 2AlCl_3$ could be obtained. Electrochemical studies of this system indicated that interconversion among the various species upon reduction is rather slow, an observation reflecting the low levels of $Al_2Cl_7^-$ present as well as the unbuffered nature of the melt in this region.

INTRODUCTION

Recent work in this laboratory has involved the characterization of aluminum chloride:alkylpyridinium chloride molten salt systems as solvents for chemical and electrochemical studies. The advantages of such solvents include the absence of moisture and the stabilization of radical species.[1-8] Evidence of interaction between the acidic $AlCl_3$:butylpyridinium chloride (BuPyCl) melt (molar excess of $AlCl_3$) and aromatic amines, forming amine-$AlCl_3$ complexes,[8] and aromatic hydrocarbons, involving oxidation of certain hydrocarbons to their cation radicals,[7] has been obtained in previous studies; in the basic melt (molar excess of BuPyCl), these species apparently exist in the uncomplexed forms. Given the well-known dependence of the electrochemical behavior of quinones upon the acid-base properties of solvent systems,[9-19] it was decided to study the electrochemistry of 9,10-anthraquinone in $AlCl_3$:BuPyCl melts of various compositions in order to relate the observed behavior to that seen in other solvent systems. Of particular interest in this comparison is the electrochemical behavior of chloranil (tetrachloro-p-benzoquinone) in the $AlCl_3$:NaCl melt,[20] which was found to involve extensive interaction of the basic NaCl:$AlCl_3$ melt with reduced quinone species (ECE mechanism). The results of the present study of 9,10-anthraquinone in the $AlCl_3$:BuPyCl system are reported herein.

EXPERIMENTAL

Cyclic voltammetric and coulometric experiments were carried out using a PAR 173 Potentiostat/Galvanostat equipped with a PAR 179 Digital Coulometer, a PAR 175 Universal Programmer, and a Houston Model 2000 X-Y Recorder. A storage oscilloscope (Tektronix Model 564) was employed for chronoamperometric experiments and for cyclic voltammetry at rapid scan rates (> 500 mV/sec). Vitreous carbon (Atomergic Chemetals Corp., 3 mm diameter, sealed in Pyrex) was used as the working electrode material in this study; the reference electrode, auxiliary electrode, and cell design have been previously described.[21] In order to avoid leakage of the 2:1 acidic melt from the reference and auxiliary compartments into the cell during experiments in the neutral melt, a Fisher Remote Reference Junction (Fisher Scientific Co., Cat. No. 13-639-55) was employed as the reference electrode compartment, while a fritted tube (Ace Glass Co., Porosity E, 4-8 μm) placed in an outer Pyrex tube having a 2 mm hole approximately 1 cm above the frit for solution contact, was used as the auxiliary electrode compartment. Experiments were conducted in a Vacuum Atmospheres Co. drybox in which the oxygen and moisture levels were typically below 2 ppm, as monitored by a Couloximeter Trace Oxygen Monitor, Model 10-100A (Chemical Sensor Development, Inc., Torrance, CA) and a Beckman Model 340 Portable Trace Moisture Analyzer (Beckman Instruments, Fullerton, CA), respectively. The atmosphere (argon) sampling stream was provided by a small pump (Air Pumper, Markson Scientific Co.) located inside the drybox; after passing through the instruments, connected in parallel, the gas stream

was vented to the laboratory exhaust system.

Preparation and purification of n-butylpyridinium chloride (BuPyCl) and aluminum chloride, as well as melt preparation, have been previously reported.[21] 9,10-Anthraquinone (denoted as AQ; Eastman Kodak Co.) was recrystallized from benzene/absolute ethanol and its purity verified by melting point and infrared spectrum. 9,10-Anthrahydroquinone (9,10-AHQ) was prepared by dithionite reduction of AQ according to the procedure of Grandmougin;[22] nitrogen was bubbled through the solvents employed in various stages of the preparation due to the air-sensitive nature of 9,10-anthrahydroquinone.

Experiments in the acidic and basic melts were carried out at melt compositions $AlCl_3$:BuPyCl of 1.2:1 and 0.8:1, respectively; studies in the neutral melt involved melt preparation by addition of equimolar quantities of $AlCl_3$ and BuPyCl and further adjustment of melt acidity through the neutral range by small additions of $AlCl_3$ or BuPyCl to the melt. At AQ concentrations above approximately 10 mM in the 1.2:1 acidic melt, precipitation of a yellow solid from the melt was observed. This solid was isolated for further study by centrifuging (Fisher Safety Centrifuge), decanting the melt above the solid, and three-fold washing of the solid with methylene chloride (dried over Type 4Å molecular sieves), centrifuging between washes. The resulting bright yellow solid was analyzed for chloride by addition of 50-70 mg of the solid to 150 ml of distilled water and argentometric titration, followed by potentiometry using a silver wire indicator electrode (%Cl found: 43.5, 44.8, 44.7, 44.8, 44.8; %Cl theoretical for $C_{14}H_8O_2 \cdot 2\ AlCl_3$: 44.8).

Infrared spectra of AQ in melts of varying acidity were obtained on a Perkin-Elmer 621 Grating Infrared Spectrophotometer using AgCl cells (0.1 mm pathlength, Wilks Scientific Company) or polyethylene film as cell materials. Cyclic voltammetry and normal pulse voltammetry were used to characterize the AQ species present at the various acidities. Since the temperature of the cell in the infrared beam was found to be considerably higher than 40°C (normally used for electrochemical studies), samples for infrared analysis were taken at 80°C in order to increase the concentration of species in solution and maximize the sensitivity of the infrared procedure; cyclic voltammetric curves were similar to those obtained at 40°C. Infrared spectra of the yellow solid isolated from the acidic melt were run as paraffin oil and hexachlorobutadiene mulls (to allow coverage of the usual infrared range) on NaCl plates. Visible spectra were obtained on a Cary 17 Ultraviolet-Visible Spectrophotometer.

RESULTS AND DISCUSSION

General Aspects and Infrared Spectroscopy

The general aspects of anthraquinone electrochemistry in the $AlCl_3$:BuPyCl melt are illustrated in the series of cyclic voltammograms shown in Figure 1, which portrays the change of electrochemical behavior observed as the melt composition, starting from a 0.8:1 $AlCl_3$:BuPyCl basic melt, was made increasingly acidic by addition of $AlCl_3$. From these voltammograms, it can be seen that the potential which is characteristic of anthraquinone reduction shifts to considerably more positive values as the melt acidity is increased. In addition, there are apparently three different species involved over the range of melt compositions studied: one each in the basic and acidic melts (top and bottom curves in Figure 1, respectively) and another, apparently intermediate species, in the neutral melt. By very careful addition of small amounts of $AlCl_3$ to the melt, a cyclic voltammogram containing all three of these reduction processes could be obtained. Similar behavior can be seen in the return sweep (oxidation scan) of the cyclic voltammograms, there being again three distinct regions of anodic activity. The electrochemical aspects of these processes will be dealt with individually (according to melt composition) in greater detail in following sections.

The nature of the various species being reduced in the melt was ascertained primarily by infrared spectroscopy. The favorable absorption window of the butylpyridinium cation in the carbonyl region[23] and the strength of the carbonyl absorption of anthraquinone enabled the effect of increasing melt acidity upon the carbonyl bonds to

be investigated (see Experimental Section). Thus, the infrared spectrum of anthraquinone in the acidic melt revealed no absorption at the usual value for the carbonyl stretching frequency (1680 cm^{-1}); however, a new band (not seen in the spectrum of the acidic melt itself) appeared at 1550 cm^{-1} (Figure 2). This is in good agreement with work carried out by Giallanardo[24] in which a yellow bis-$AlCl_3$-AQ complex (structure confirmed by elemental analysis for C, H, and Ag^+ titration for Cl^-), was precipitated from methylene chloride and found to have no absorption at the normal carbonyl frequency but exhibited a shifted band at 1550 cm^{-1}; thus, it seems probable that the species present in the acidic melt is the bis-$AlCl_3$-AQ complex, the complexation occurring at the carbonyl functions. Further proof of this characterization was obtained by raising the concentration of AQ in the acidic melt sufficiently to cause precipitation of a yellow solid from the melt. After centrifuging and both before and after washing with methylene chloride (thus reducing and then entirely eliminating absorption contributions from butylpyridinium cation), the infrared spectrum of this compound proved to be identical to the entire spectrum published[24] for the isolated bis-$AlCl_3$-AQ complex. Furthermore, chemical analysis of the isolated complex by argentometric titration for chloride indeed showed the existence of two $AlCl_3$ molecules for each AQ molecule.

The infrared spectrum of the neutral melt containing AQ (similar in composition to that corresponding to the fourth scan in Figure 1) revealed bands at both 1680 and 1550 cm^{-1} (Figure 2); this observation is in accordance with the absorption expected of a mono-$AlCl_3$-AQ

complex.[24] Finally, the infrared spectrum of AQ in the basic melt has a band at 1680 cm^{-1}, but not at 1550 cm^{-1}, thus indicating that the AQ carbonyl group exists in the uncomplexed form in the basic melt. The visible absorption spectrum of 9,10-anthraquinone in the basic melt revealed one band at 330 nm (ε = 5,210, c.f. λ_{max} = 326 nm, ε = 5,800 in DMF[19]), while the spectrum in the acidic melt showed absorptions at 335 nm (ε = 9,660) and 440 nm (ε = 6,970). It has been previously observed that mono-protonation of 9,10-anthraquinone in sulfuric acid results in a spectrum containing absorbances at 311 nm and 410 nm,[25-26] again supporting the complexation of anthraquinone by $AlCl_3$ in the acidic melt; apparently, the formation of a bis-$AlCl_3$-AQ complex ($AQ \cdot 2AlCl_3$) accounts for the increased bathochromic shift (to 440 nm), relative to that for mono-protonated AQ above, observed for 9-10-anthraquinone in the acidic melt. It should be noted that the formation of the AQ-$AlCl_3$ complexes is chemically reversible; that is, if an acidic melt containing AQ is made basic, a shift of electrochemical behavior to that characteristic of AQ in the basic melt is observed. The interaction of $AlCl_3$ with AQ appears, then, to account for the observed shifts in the potential of AQ reduction as melt acidity is varied.

A comparison of the potential observed for AQ reduction in the basic melt with those found in other solvents may be made by noting that the 2:1 $AlCl_3$:BuPyCl reference electrode used in the molten salt system is 60 mV positive of the saturated calomel electrode (using for comparison the ferrocene-ferrocenium redox potential in the melt and acetonitrile solutions[7]); the potential for 9,10-AQ reduction in the basic melt is, then approximately -550 + 60 = -490 mV vs. SCE.

This value appears to be closer to values observed for 9,10-AQ reduction in protic solvents (-575 and -580 mV vs. SCE in 75% aqueous dioxane[16] and 20% aqueous acetonitrile,[27] respectively) than those found in aprotic solvents (-980 and -930 mV vs. SCE in acetonitrile and dimethylformamide, respectively, for reduction of AQ to the anion radical[13]); this, together with other evidence (vide infra), seems to indicate extensive interaction of the melt with the reduced AQ, as is observed in protic solvents. 1,4-Benzoquinone, for which a peak potential for reduction in the basic melt of -185 mV (vs. SCE, calculated as above) was found, underwent decomposition as the melt acidity was increased past the neutral point and was not further investigated. The positive shift of 0.6 V observed for AQ reduction upon mono-complexation with $AlCl_3$ correlates rather well with the shift (approx. 0.6V) observed for AQ reduction upon mono-protonation in several nonaqueous solvents.[13] Complexation of the carbonyl oxygen by $AlCl_3$ would result in a withdrawal of charge from the 9,10-AQ ring system through the carbonyl bond, leading both to a positive shift in reduction potential and a reduction in the carbonyl bond order, as evidenced by the marked decrease in carbonyl stretching frequency observed as melt acidity is increased.

It is of some interest to compare the results of the present study with earlier work involving organic species in the $AlCl_3$:BuPyCl melts. In a study of aromatic amines,[8] $AlCl_3$ complexation of the amines in the acidic melt was found to shift the potential for amine-cation radical oxidation to more positive values; in the case of N,N,N',N'-tetramethylbenzidine (containing two amino functions), three distinct species, assumed to be the free amine, the mono-$AlCl_3$

amine complex, and the bis-$AlCl_3$ amine complex, were evident in the cyclic voltammetric scans as the acidity of the melt was increased. The potential shift of the oxidation process for this benzidine also amounted to +1.4 V over the base-acid acidity range, indicating that approximately the same degree of alteration of electron density by $AlCl_3$ complexation occurs as seen with 9,10-AQ. A study of various aromatic hydrocarbons in the $AlCl_3$:BuPyCl melt[7] also indicated some interaction of $AlCl_3$ with the aromatic systems. The above studies indicate that, although excess $AlCl_3$ exists as $Al_2Cl_7^-$ in the acidic melt, the interaction between $AlCl_3$ and $AlCl_4^-$ (forming $Al_2Cl_7^-$) is not so strong as to prevent the displacement of $AlCl_4^-$ from $Al_2Cl_7^-$ by species possessing a reasonable amount of electron-donating ability. Since the amount of free $AlCl_3$ is small even in very acidic melts,[5] this situation may be likened to that involving the existence of the proton in aqueous solution as the hydronium ion H_3O^+ rather than as the free proton; interaction of basic species with the hydronium ion by displacement of an H_2O molecule is analogous, then, to the displacement reaction described above involving $Al_2Cl_7^-$ and $AlCl_4^-$.

Electrochemical Behavior in Basic Melt

The electrochemical behavior of AQ in the basic melt, in which the AQ exists in the uncomplexed form, was further investigated by coulometric reduction at -0.800 V, resulting in an n-value for the reduction of 2.0. Cyclic voltammetry of the reduced species (initial potential -0.300 V, initial cathodic scan) showed that the long-term reduction product (i.e., coulometry product) was identical to that observed in the cyclic voltammetry of AQ, since an anodic peak at

0.00 V was seen in the first positive sweep, the following negative sweep again showing a cathodic reduction peak at -0.55 V due to reduction of AQ. Coulometric oxidation at +0.100 V in the above melt was also found to involve two electrons; a cyclic voltammogram following oxidation (same conditions as Figure 1) was identical to that in Figure 1 (first scan). A Nernst plot obtained by varying the ratio of AQ to AQ dianion by coulometric reduction and measurement of the corresponding potentials revealed a slope of 31 mV per decade of the above ratio (Figure 3), indicating that AQ and its dianion comprise a potentiometrically reversible two-electron system. Addition of an authentic sample of anthrahydroquinone to a basic melt gave rise to cyclic voltammetric behavior identical to that observed above following coulometric reduction. The anthrahydroquinone, upon addition to the melt, presumably is converted into a complexed dianion by interaction with species in the melt (i.e., $AlCl_4^-$) with the consequent release of two protons, as has been observed upon the addition of tetrachloro-p-benzohydroquinone to the $AlCl_3$:NaCl melt;[20] however, in the $AlCl_3$:BuPyCl basic melt, proton reduction is rather ill-defined and occurs near the cathodic limit[6] so that direct observation of proton reduction was not possible. Solutions of both AQ and electrogenerated dianion were found to be stable for several days in the basic melt; thus, the overall aspects of electrochemical reduction of AQ to the dianion and oxidation of this species back to the quinone appear to be quite straightforward.

Previous studies of quinone reduction in various media have shown that the electrochemical behavior observed depends upon the

extent of association of the quinone reduction products (anion radical and dianion) with species capable of complexing (protonating as a special case) these anions. In aprotic media (i.e., absence of protons), two successive one-electron reversible systems corresponding to the quinone/quinone anion radical and quinone anion radical/quinone dianion redox systems are observed, while the addition of a proton source (water, various acids) to these media causes a positive shift of the redox systems, the magnitude of the shifts depending on concentration and type of proton donor employed.[12-14] Under conditions of high proton availability (aqueous systems, high concentration of proton donor) a single two-electron process is observed.[9-11,16,17] The various possible mechanisms under these conditions have been summarized by a number of authors;[11,13,14,17] the different pathways involve different sequences of protonation and electron transfer. In the present study, then, the observation of a single two-electron reduction process indicates a strong interaction between the anion radical and the melt, this interaction being rather rapid and irreversible since no additional peaks were noted in the cyclic voltammograms at scan rates up to 5 V/sec. The wide separation in potentials for the reduction and oxidation peaks, observed here for AQ in the basic melt (600 mV), has also been noted previously and ascribed to the irreversible protonation of the quinone dianion (or anion radical) following reduction.[13] Considering the species present in the basic melt, the most likely mechanism for this interaction is displacement of Cl^- from $AlCl_4^-$ by the oxygen anion, leaving the reduced quinone species effectively complexed by $AlCl_3$. Recent work concerning the

interaction of oxide ions with $AlCl_3$:NaCl melts involves an analogous mechanism in which the oxide ion acts as a dibase, displacing two Cl^- ions from $AlCl_4^-$ present in the melt.[28] Assuming this general type of interaction for the reduced AQ species, the overall equilibrium between AQ and the AQ dianion in the basic melt can be written, recalling that the evidence indicates that AQ is uncomplexed in the basic melt,

$$AQ + m\ AlCl_4^- + 2e^- \rightleftarrows AQ\ (AlCl_3)_m^{=} + m\ Cl^-,$$

with the corresponding Nernst equation

$$E = E^\circ + \frac{RT}{2F} \ln \frac{[AQ]}{[AQ(AlCl_3)_m^{=}]} + \frac{mRT}{2F} \ln \frac{[AlCl_4^-]}{[Cl^-]} .$$

This relationship was examined experimentally by carrying cut a coulometric reduction of AQ (passing one equivalent of electricity to produce an equimolar mixture of AQ and AQ dianion) in an initially slightly basic melt (0.95:1) and measuring the equilibrium potential at a glassy carbon electrode after successive additions of BuPyCl. The resulting Nernst plot was linear (Figure 4), with a slope of 80 mV (theoretical slope, 31 mV for m = 1), thereby confirming the involvement of two $AlCl_4^-$ ions with the AQ dianion, with some involvement by a third $AlCl_4^-$. Further evidence for dianion complexation was obtained from the visible absorption spectrum of coulometrically-produced AQ dianion in the basic melt. When compared with literature spectra for reduced AQ species in various solvents, this spectrum, having maxima at 425 nm (ε = 4,970) and 380 nm (ε = 6,570) was found to be most similar to that of anthrahydroquinone (420 nm, 384 nm in DMF), and not that of the free dianion (503 nm, ε = 13,900).[19] Considering that anthrahydroquinone is actually the AQ dianion complexed

by two protons, the similarity of the spectra seen above strongly indicates that the AQ dianion in the basic melt is also complexed by at least two acidic species (i.e., $AlCl_3$). It is interesting to note that studies by Peover and Davies on lithium ion complexation of anionic intermediates in AQ reduction[29] indicate that the AQ dianion is complexed by an average number of 2.3 lithium ions, thus providing additional evidence for the ability of a single oxygen anionic site to interact with more than one acidic species.

As can be seen from Figure 1, the reduction peak for AQ in the basic melt is quite broad, the E_p-$E_{p/2}$ value being ~100 mV, considerably larger than that characteristic of a reversible two-electron process at 40°C (31 mV). Further investigation of this process by normal pulse voltammetry (Figure 5) revealed a small maximum on the voltammogram, probably due to reactant adsorption (that is, adsorption of AQ at glassy carbon), as studied previously by other workers.[30,31] Reversal of the potential scan past the maximum resulted in a virtual retracing of the forward scan (with maximum), thus eliminating such effects as product filming and depletion of reactant at the electrode surface (vide infra) as causes for the maximum. An increase in pulse width led to a decrease in the size of the maximum, an effect noted by Anson et. al.[31] Reverse pulse polarography of AQ in the basic melt (Figure 5) (scanning anodically from an initial potential of -0.80 V) indicated that the dianion apparently does not adsorb at the electrode surface, there being no maximum on the voltammogram; the extensive interaction of the melt with the dianion (vide supra) may account for this behavior.

In the course of obtaining normal pulse voltammograms for AQ reduction in the basic melt, it was found that the nature of the voltammogram

varied markedly depending upon the initial potential employed. At an initial potential of +0.200 V, a value positive of the peak potential for the anodic process (Figure 1), the usual type of normal pulse voltammetric curve is obtained, the small maximum having already been described. As the initial potential was made increasingly negative, so that restoration of the initial AQ concentration by oxidation between pulses of quinone reduced during pulses is decreased, and then eliminated, the normal pulse voltammetric responses underwent a sharp decrease with pronounced maxima also being observed; reversal of the potential scan past the maximum resulted in a continuous decrease in reduction current, as opposed to the case involving adsorption above. This general behavior has been reported by Oldham and Parry as being characteristic of a depletion effect observed in normal pulse polarography when initial concentration conditions are not restored between pulses.[32] The observation of such an effect is certainly not surprising in view of the high viscosity of the present system (23.5 cP for 1:1 melt at 40°C[7]) compared to that of aqueous systems (0.653 cP at 40°C[33]); thus, judicious choice of initial potential for normal pulse voltammetry in the organic melts is evidently of great importance in obtaining useful normal pulse voltammetric data.

Consideration of a detailed mechanism for the reduction process within the scheme given by Jeftic and Manning[13] must involve the sequence of electron transfers and $AlCl_3$ complexation steps, the point of interest being whether the anion radical is complexed immediately after its formation or complexation occurs only after the second electron transfer. Both types of behavior have been observed by various authors for AQ

reduction in aprotic solvents containing proton donors.[12,34] Extending these investigations to other Lewis acids, a significant degree of interaction of lithium ion with the AQ anion radical has been observed in dimethyl-formamide solution, although the interaction with the dianion is much stronger (vide supra).[29] Similar studies on naphthoquinone reduction in the presence of several metal cations showed that the extent of complexation of the anion radical by the cations increased as the charge on the metal ion increased;[35] thus, it seems reasonable to assume that the AQ anion radical is complexed rather extensively (and apparently fairly rapidly) in the basic melt. This complexed anion radical should be more easily reducible than the quinone,[36] leading to an ECE process; alternatively, a single electron transfer followed by disproportion of the complexed anion radical (second-order kinetics) should also be considered. A single-wave two-electron process would be observed in either case. Distinction between the kinetic reaction orders involved can be made on the basis of concentration dependence of peak current functions except when the following chemical reaction is extremely rapid,[37] when this dependence for the two cases becomes identical. That a rapid chemical reaction is involved in the present case has already been suggested by the cyclic voltammetric behavior observed and was confirmed from the results of a single-step chronoamperometric experiment (potential stepped from -0.300 to -0.800 V), in which a linear plot of current vs. $t^{-1/2}$ was obtained over a time range of 10 msec to 5 sec.[38] In the case of electrode reactions involving rapid chemical kinetics, Saveant has suggested that the extent of peak potential shift as a function of scan rate can be used as a criterion for distinguishing

between first and second order kinetics, the shifts being 29 mV and 19 mV (20°C), respectively, per decade scan rate change.[37,39] The experimentally observed shift of 80 mV, however, is probably due mostly to the effects of slow charge transfer; therefore, definitive evidence for either reaction path is lacking. Consideration of the chemical reactivity of the basic melt toward the reduced quinone species tends to favor the ECE path,[37] since production of high concentrations of the complexed intermediate would encourage a second electron transfer. The mechanism for the reduction process can be tentatively written as

$$AQ + 1e^- \rightleftarrows AQ^{\cdot-}$$

$$AQ^{\cdot-} + AlCl_4^- \rightarrow AQ(AlCl_3)^{\cdot-} + Cl^-$$

$$AQ(AlCl_3)^{\cdot-} + 1e^- \rightleftarrows AQ(AlCl_3)^{=}$$

$$AQ(AlCl_3)^{=} + AlCl_4^- \rightleftarrows AQ(AlCl_3)_2^{=} + Cl^-$$

with some partial complexation by a third $AlCl_3$, as indicated by the Nernst plot slope.

The irreversible nature of the first complexation step was deduced from the wide separation in potentials observed for the reduction and oxidation processes in the basic melt; from Figure 1, the oxidation process occurs in the same potential region as does the reduction of the mono-$AlCl_3$ AQ complex. This behavior indicates that the oxidation of the complexed quinone dianion in the basic melt involves a mono-$AlCl_3$ complex which is not at equilibrium during the oxidation process. Upon raising the temperature to 110°C, cyclic voltammetry in the quinone solution (200 mV/sec scan rate) showed only small peak potential shifts for the reduction and oxidation processes, again demonstrating the irreversibility of the complexation reaction.

Electrochemical Behavior in Neutral Melt

As the melt is made more acidic, another process is observed at +0.00 V, corresponding to reduction of the AQ·$AlCl_3$ complex. As shown in Figure 1 (second scan), if the melt basicity is such that a certain amount of electroactivity due to the uncomplexed AQ is also present (i.e., neutral-basic melt), the reduction of the AQ·$AlCl_3$ complex apparently proceeds in two one-electron steps since two components, separated by about 100 mV, are visible in the broad reduction peak. With a slight increase in melt acidity or decrease in scan rate, the individual components in the reduction peak merge into a single peak (scans 3 and 4 in Figure 1) and the behavior begins to resemble that of a reversible system (approximately equal reduction and oxidation peak heights, 100 mV peak separation). Since coulometry in the neutral melt is not feasible due to slow equilibration among the quinone complexes (vide infra), an approximate n-value for AQ·$AlCl_3$ reduction in the neutral melt (as in scan 4, Figure 1) was obtained from normal pulse voltammetric data using diffusion coefficients found from the AQ-$Al_2Cl_7^-$ titration experiment (vide infra). This procedure led to an n-value of 2.3 for AQ·$AlCl_3$ reduction which, considering the approximations involved, indicates a two-electron reduction. Although Hale and Parsons have shown the possibility, in the case of protonated quinones, of successive charge transfers (forming anion radical and dianion) at the same potential, without involving disporportionation or intermediate chemical reactions (ECE case),[40] the effects of scan rate and melt

acidity on the nature of the reduction process in this case seem to indicate the presence of coupled chemical reaction between charge transfers:

$$AQ(AlCl_3) + 1e^- \rightleftarrows AQ(AlCl_3)^{\cdot}$$

$$AQ(AlCl_3)^{\cdot} + AlCl_4^- \rightleftarrows AQ(AlCl_3)_2^{\cdot} + Cl^-$$

$$AQ(AlCl_3)_2^{\cdot} + 1e^- \rightleftarrows AQ(AlCl_3)_2^{=}$$

$$AQ(AlCl_3)_2^{=} + AlCl_4^- \rightleftarrows AQ(AlCl_3)_3^{=} + Cl^-.$$

The increased degree of reversibility of this system compared to that in the basic melt can probably be ascribed to the prior complexation of the AQ as $AQ{\cdot}AlCl_3$ in the neutral melt, since reduction of $AQ{\cdot}AlCl_3$ would yield a complexed anion radical, $AQ{\cdot}AlCl_3^{\cdot}$. Thus, the same molecular structure exists before and after e-transfer to form the complexed anion radical; if the following chemical reactions and electron-transfer are reversible, then, reversible behavior should be observed for the system as a whole. Two effects stemming from the increased acidity of this medium should also be noted: first, the chemical species involved in the equilibria above should also include $Al_2Cl_7^-$ to some extent, since the concentration of this species begins to increase rapidly in the neutral region, and second, the final equilibrium in the series forming $AQ(AlCl_3)_3^{=}$ should be rather complete (as opposed to the partial complexation in the basic melt).

As the melt acidity is increased, the reduction of the $AQ{\cdot}2AlCl_3$ complex (2nd and 3rd CV's) at +0.8 V becomes evident. In addition, the oxidation processes also shift to more positive potentials, suggesting successively higher complexation of the quinone dianion; thus, the

species $AQ(AlCl_3)_1^=$, $AQ(AlCl_3)_2^=$, and $AQ(AlCl_3)_3^=$ would account for the oxidation peaks observed. As seen in the third CV in Figure 1, in which $AQ(AlCl_3)$ is the major species, the following chemical reactions become more irreversible as melt acidity increases, thus increasing the amount of dianion oxidized as $AQ(AlCl_3)_2^=$ rather than $AQ(AlCl_3)_1^=$ after $AQ(AlCl_3)$ reduction.

The attainment of equilibrium among the various quinone complexes as reduction proceeds is evidently rather slow, since the relative cyclic voltammetric peak heights for reduction of the three quinone species were found to be essentially constant as a function of scan rate. Normal pulse voltammetry of the complexes in the neutral melt clearly showed the presence of three species over the pulse width range of 20 msec to 750 msec, thus indicating again the slow equilibrium among the species; however, the height of the wave due to $AQ \cdot 2AlCl_3$ reduction (most positive wave) was found to increase relative to those due to reduction of $AQ \cdot AlCl_3$ and AQ as the pulse width was increased. The situation apparently corresponds, then, to the case of an electron transfer preceded by a homogeneous chemical reaction, for which an increase in current, relative to that observed for diffusion only, would be expected.[41] The reduction step occurring at the most positive potential, for example, corresponds to the two-electron reduction of $AQ \cdot 2AlCl_3$, the preceding chemical reaction being the complexation of $AQ \cdot AlCl_3$ by $Al_2Cl_7^-$ (i.e., first-order in each species) in response to depletion of $AQ \cdot 2AlCl_3$ by the reduction process; a similar relationship between $AQ \cdot AlCl_3$ and AQ should also hold. The current-time behaviors of the various reduction processes were examined by means of a log i vs.

log t (t = pulse width) plot for each process (Figure 6), from which slope values $\alpha(i = kt^{\alpha})$ of -0.44, -0.47, and -0.74 for reduction of $AQ \cdot 2AlCl_3$, $AQ \cdot AlCl_3$, and AQ were obtained. When compared to an α value of -0.50 for a purely diffusional process, these values indicate a current decrease less than that expected for diffusion involving reduction of $AQ \cdot 2AlCl_3$ (again indicating a shift in equilibrium toward the $AQ \cdot 2AlCl_3$ complex), while the current-time decrease for uncomplexed AQ is substantially larger than that expected for purely diffusional current-time behavior, reflecting a decrease in AQ concentration as the complexation equilibria shift toward the $AlCl_3$ complexes reduced previously. The α value observed for $AQ \cdot AlCl_3$, being close to 0.50, would seem to affirm the intermediate nature of this complex; that is, the concentration of $AQ \cdot AlCl_3$ evidently remains relatively constant since it is formed from AQ by $AlCl_3$ complexation but depleted by further complexation to form $AQ \cdot 2AlCl_3$. The slow rate of interconversion among the complexes observed above may be due to the limited availability of $Al_2Cl_7^-$ in the neutral melt (since it is unbuffered with respect to $Al_2Cl_7^-$) and not to unusually low rate constants for the complexation reactions themselves.

The equilibria involving complexation of AQ by $Al_2Cl_7^-$

$$AQ + Al_2Cl_7^- \overset{K_1}{\rightleftharpoons} AQ \cdot AlCl_3 + AlCl_4^-$$

$$AQ \cdot AlCl_3 + Al_2Cl_7^- \overset{K_2}{\rightleftharpoons} AQ \cdot 2AlCl_3 + AlCl_4^-$$

were studied by means of a titration of AQ, initially in a neutral melt, with an acidic melt ($AlCl_3$:BuPyCl 1.06:1.00), the titration being followed by normal pulse voltammetry (20 msec pulse width). In this procedure, the composition of the neutral melt at the beginning of the titration

was adjusted so that the presence of the AQ·$AlCl_3$ complex was barely detectable; at this point, the $Al_2Cl_7^-$ concentration was assumed to be low compared to levels found in later stages of the titration. The addition of the acidic melt titrant first caused the appearance of the wave corresponding to the AQ·$AlCl_3$ complex, requiring an amount of titrant considerably more than (approximately twice) the stoichiometric amount of AQ present. The concentration of AQ remaining was calculated by the decrease of the wave corresponding to uncomplexed AQ, leading to a value for the AQ·$AlCl_3$ concentration by difference between the original concentration of AQ and concentration of AQ remaining. The concentration of $Al_2Cl_7^-$ was obtained by subtracting the AQ·$AlCl_3$ concentration from the total amount of $Al_2Cl_7^-$ added as titrant. The concentration of $AlCl_4^-$, which is virtually constant in the neutral region, was taken as 4.05 M. A similar approach was followed for obtaining AQ·$2AlCl_3$ concentration values during the second "break" of the titration using points at which only AQ·$AlCl_3$ and AQ·$2AlCl_3$ were present; the D value used for calculating the AQ·$AlCl_3$ concentration was that obtained when only AQ·$AlCl_3$ and AQ were present during the first part of the titration. As with the first complexation, considerable excess of titrant was required to cause complete formation of the AQ·$2AlCl_3$ complex. From the above procedure, K_1 and K_2 values of 800 and 300, respectively, were found (Table 1). These values should be regarded as only approximate ($\pm$ 25%) since the method assumes that the D values for the various AQ species remain constant during the titration, while in fact the changing composition of the melt may cause considerable variation in these values. No attempt was made to include activity coefficients in the equilibrium equations.

Since the protonation of AQ has been studied by numerous authors in connection with the Hammett acidity scale, it is possible, at least in a qualitative sense, to relate the acidity of the $AlCl_3$:BuPyCl solvent system to the Hammett scale. Using the value of K_1 obtained above, the concentration of $Al_2Cl_7^-$ in a melt containing equal amounts of AQ and AQ·$AlCl_3$ is found to be approximately 5 mM, while protonation of AQ in sulfuric acid-water mixtures has been observed to occur at a Hammett value of approximately 8.6.[26] While the Hammett scale is based upon protonation as opposed to $AlCl_3$ complexation, this comparison qualitatively indicates that the $AlCl_3$:BuPyCl solvent system begins to exhibit highly acidic properties even at relatively small values of $Al_2Cl_7^-$ concentration. The ease with which AQ·$AlCl_3$ is further complexed to form AQ·$2AlCl_3$ is additional evidence of this great acidity.

Electrochemical Behavior in Acidic Melt

As seen in Figure 1, the electrochemical behavior of AQ in the acidic melt is similar to that observed in the basic melt in that the oxidation and reduction processes are separated by some 500 mV; as mentioned previously, the potential shift of +1.4 V for the system as a whole, with respect to the system in the basic melt, is due to complexation of AQ as AQ·$2AlCl_3$. The cathodic process again involves the two-electron reduction of the complexed AQ to the quinone dianion, as established by coulometry of AQ in the acidic melt at +0.50 V and comparison of cyclic voltammograms of the final coulometry mixture and of a melt containing authentic anthrahydroquinone (identical oxidation peak potentials). Subsequent coulometric oxidation of the dianion revealed that the anodic process corresponds to two-electron oxidation back to AQ·$2AlCl_3$, the cyclic

voltammetric behavior of the oxidized species in the coulometry melt being identical to that of $AQ \cdot 2AlCl_3$ in the acidic melt. As in the basic melt, a Nernst plot of potential vs. $\log_{10}$ of the ratio of $AQ \cdot 2AlCl_3$ to its coulometrically produced reduction product (slope = 29 mV) indicated a reversible two-electron process. Since charge transfer is apparently rather rapid in the acidic melt (vide infra), the peak potential separation observed for the cathodic and anodic processes implies that, as in the basic melt, an irreversible chemical reaction following reduction is responsible for the lack of reversibility in the system as a whole. The quinone/quinone dianion redox equilibrium including chemical interaction of $Al_2Cl_7^-$ ions with the dianion (since $Al_2Cl_7^-$ should be more reactive than $AlCl_4^-$ toward oxyanions) can be written as

$$AQ \cdot (AlCl_3)_2 + mAl_2Cl_7^- + 2e^- \rightleftarrows AQ(AlCl_3)_{2+m}^{=} + mAlCl_4^-,$$

and the corresponding Nernst equation as

$$E = E^\circ + \frac{RT}{2F} \ln \frac{[AQ(AlCl_3)_2]}{[AQ(AlCl_3)_{2+m}^{=}]} + \frac{mRT}{2F} \ln \frac{[Al_2Cl_7^-]}{[AlCl_4^-]} .$$

A Nernst plot obtained in an acidic melt containing equimolar amounts of $AQ \cdot 2AlCl_3$ and its dianion and varied in $\frac{[Al_2Cl_7^-]}{[AlCl_4^-]}$ by incremental addition of $AlCl_3$ was found to have a slope of 60 mV per decade change in $\frac{[Al_2Cl_7^-]}{[AlCl_4^-]}$, indicating that two $Al_2Cl_7^-$ ions are involved in chemical reactions following $AQ \cdot 2AlCl_3$ reduction. Visible absorption spectroscopy of a solution of coulometrically-produced dianion revealed absorption maxima at 400, 380, and 360 nm (ϵ=8,760; 9,120; 5,470, respectively) showed a blue shift relative to the spectrum obtained in the basic melt. Since previous studies in other systems[19] have indicated that protonation of the AQ dianion to form the hydroquinone (the spectrum of which is

very similar to that of the dianion in the basic melt) causes a blue shift in the visible spectra, the further blue shift observed in the present case seems to support the existence of the dianion in the acidic melt as $\bar{AQ}(AlCl_3)_4^{=}$.

From the cyclic voltammogram in Figure 1, it is apparent that the reduction peak for AQ in the acidic melt is much sharper ($E_{p/2} - E_p$ = 40 mV at 200 mV/sec scan rate; theoretical $E_{p/2} - E_p$ = 31 mV for n = 2 at 40°C[42]) than that in the basic melt ($E_{p/2} - E_p \cong 80$ mV). At lower scan rates (~20 mV/sec), $E_{p/2} - E_p$ values approached the theoretical value, probably indicating the effects of uncompensated cell resistance at higher scan rates (vide infra); therefore, it appears that a two-electron reversible process is involved for AQ reduction in the acidic melt. Normal pulse voltammetric data for $AQ \cdot 2AlCl_3$ reduction (initial potential + 1.20 V) supported this conclusion, the observed slope of an E vs. log $\frac{i_d - i}{i}$ being 40 mV/log unit; from the i_d value, a diffusion coefficient of 2.6 $\pm$ 0.1 x 10^{-7} cm^2/sec was found for $AQ \cdot 2AlCl_3$ reduction in the 1.2:1.0 melt, compared to a value of 6.2 $\pm$ 0.2 x 10^{-7} cm^2/sec for AQ reduction in the basic (0.8:1.0) melt. The presence of rapid chemical reactions coupled with the charge-transfer process was deduced from the cyclic voltammetric behavior at scan rates higher than 5 V/sec, beyond which an additional cathodic and anodic process (at +0.34V and +0.97V, respectively; 20 V/sec scan rate) began to appear. As in the basic melt, an i vs. $t^{-1/2}$ plot for chronoamperometric data was found to be linear over a time frame of 10 msec to 5 seconds, again indicating very rapid chemical kinetics.

Further investigation of the electrode process involved elucidation of the order of the chemical reaction coupled to the charge transfer

reaction. A linear dependence of cyclic voltammetric peak currents (at scan rates of 20 and 200 mV/sec), as well as of normal pulse voltammetric limiting currents (40 msec pulses), upon concentration (0.10 mM - 0.90 mM) was observed in the acidic melt; however, as mentioned previously, both first and second order mechanisms are consistent with this behavior when the following chemical reaction is very rapid.[37] Since this was shown to be the case, the criteria of Saveant involving peak potential-scan rate dependence[37,39] was employed. The experimental value of E_p shift with scan rate, observed over the range 2-500 mV/sec, was found to be 25 $\pm$ 2 mV per decade scan rate increase, which, when corrected for the effects of uncompensated cell resistance (by subtracting peak shift observed for ferrocene reduction, approximately 4 mV/$\log_{10}$ scan rate) places the value in the range 20-24 mV. Thus, this value, when compared to the theoretical values of 31 and 21 mV (40°C) for first and second order processes,[39] seems to indicate the presence of a second-order reaction coupled to the charge-transfer process for AQ reduction in the acidic melt. On this basis, the reduction mechanism can be written:

$$AQ(AlCl_3)_2 + 1e^- \rightleftarrows AQ(AlCl_3)_2^{\cdot-}$$

$$AQ(AlCl_3)_2^{\cdot-} + Al_2Cl_7^- \rightleftarrows AQ(AlCl_3)_3^{\cdot-} + AlCl_4^-$$

$$2\ AQ(AlCl_3)_3^{\cdot-} \rightleftarrows AQ(AlCl_3)_4^{=} + AQ(AlCl_3)_2$$

disproportionation being thermodynamically feasible for the further complexed anion radical $AQ(AlCl_3)_3^{\cdot-}$. Although several alternative mechanisms, each involving a second-order step, have been suggested by Feldberg[43] and Saveant,[39] the above mechanism is considered to be the most likely, since some evidence of an interaction of the melt with the

anion radical is again seen from the peak potential separation for the reduction and oxidation processes. This interaction, however, is not nearly as irreversible as that in the basic melt judging from the fact that reversible cyclic voltammetric behavior for the system as a whole is attained at higher temperature (80°C) and slower scan rate (10 mV/sec), behavior not even approached under these conditions in the basic melt. The greater reversibility of this interaction in the acidic melt is evidence that the rate of dissociation of the complexed dianion upon oxidation is much greater in the acidic melt than that in the basic melt. The higher degree of complexation, both of AQ and of AQ dianion, in the acidic melt (compared to the basic melt) may account for this difference in behavior. Since $AQ(AlCl_3)_3^-$ should be more easily reduced than $AQ(AlCl_3)_2$,[36] the fact that ECE behavior is not observed for the reduction process in the acidic melt could be explained either by assuming that the complexation equilibrium of the anion radical does not lie completely to the right or by assuming, as seems to be the case, that the disproportionation reaction of $AQ(AlCl_3)_2^-$ is rapid enough so that appreciable amounts of $AQ(AlCl_3)_3^-$ are not present near the electrode surface.

SUMMARY AND CONCLUSIONS

The electrochemical and spectroscopic behavior of 9,10-anthraquinone in the $AlCl_3$:BuPyCl molten salt system has been found to be profoundly dependent upon the acidity (that is, ratio of $AlCl_3$ to BuPyCl) of the melt, the changes in these properties arising from the complexation of AQ by $Al_2Cl_7^-$ to form successively AQ·$AlCl_3$ and AQ·$2AlCl_3$ as acidity is increased through the neutral region.

Electrochemical behavior in the basic melt, in which AQ is present in the uncomplexed form, involves an overall two-electron process and, from the appearance of the normal pulse and cyclic voltammograms, slow electron transfer. Since a strong interaction between the reduced AQ and $AlCl_4^-$ is evident both from the separation of potentials observed for reduction of AQ and oxidation of its dianion and from the visible abosrption spectrum of the dianion, an ECE mechanism is thought to be involved for AQ reduction in the basic melt. This pathway can be summarized within a diagram of the same type as used by previous authors[13,44,45] to describe quinone electrochemistry (Figure 7); in this figure, electron transfer processes are represented as occurring along the rows, while successive interactions with melt components (that is, $AlCl_4^-$ and/or $Al_2Cl_7^-$) are depicted along the columns. The ECE process for AQ reduction in the basic melt can be represented by the sequence a,r,d,v, with some reaction along path x, where r, v, and x involve interaction with $AlCl_4^-$.

The effect of $AlCl_3$ complexation in the acidic (1.2:1) melt, forming AQ·$2AlCl_3$ as established by infrared spectroscopy and chemical analysis, is a marked shift in potential (+1.4V) observed for AQ·$2AlCl_3$

reduction with respect to that seen for reduction of uncomplexed AQ in the basic melt. The interaction of $AQ \cdot 2AlCl_3$ with the melt upon reduction to form more highly complexed reduction products appears to be more reversible than is the case in the basic melt, since the cyclic voltammetric peak potential separation for the processes corresponding to reduction of $AQ \cdot 2AlCl_3$ and oxidation of the further complexed dianion decreases with an increase in temperature or a decrease in scan rate. Based on cyclic voltammetric peak potential vs. scan rate behavior for the reduction process in the acidic melt, the overall mechanism has been assumed to involve a disproportionation process, represented by the pathway e,w,dp in the diagram (Figure 7). Note that $AlCl_3$ complexation in the acidic melt has shifted the initial reduction step downwards two positions in the diagram, with the path dp intended to represent the disproportionation of $AQ(AlCl_3)_3^-$ to produce $AQ \cdot 2AlCl_3$ and $AQ(AlCl_3)_4^=$, the final product of the reduction.

The rapidly changing acidity in the neutral melt gives rise to the interesting electrochemical behavior observed for AQ in this region; that is, as acidity is varied through this region, three distinct reduction processes can be observed corresponding to reduction of uncomplexed AQ, of $AQ \cdot AlCl_3$ (inferred from infrared spectral data), and of $AQ \cdot 2AlCl_3$. It should be noted that the reduction of $AQ \cdot AlCl_3$ cannot be observed separately from the other reduction processes, an observation corresponding to the relatively small difference between equilibrium constants observed for the two $AlCl_3$ complexation steps.

In a melt containing all three complexes, it appears that the rate of interconversion among these complexes upon reduction is fairly slow, an observation reflecting the initially low levels of $Al_2Cl_7^-$ present as

well as the unbuffered nature of the melt in the neutral region. Although assignment of an exact mechanism for AQ·$AlCl_3$ reduction is very difficult, the cyclic voltammetric behavior as a function of scan rate and acidity seems to point to an ECE mechanism, as given by the sequence c,u,f,x in Figure 7.

ACKNOWLEDGEMENT

The authors gratefully ackowledge support by the Office of Naval Research and the Air Force Office of Scientific Research under Contract F49620-79-C-0142.

REFERENCES

1. Chum, H. L.; Koch, V. R.; Miller, L. L.; Osteryoung, R. A. J. Am. Chem. Soc. 1975, 97, 3264.

2. Chum, H. L.; Koran, D.; Osteryoung, R. A. J. Organomet. Chem. 1977, 140, 349.

3. Koch, V. R.; Miller, L. L.; Osteryoung, R. A. J. Am. Chem. Soc. 1976, 98, 5277.

4. Robinson, J.; Bugle, R. C.; Chum, H. L.; Koran, D.; Osteryoung, R. A. J. Am. Chem. Soc. 1979, 101, 3776.

5. Gale, R.; Gilbert, B.; Osteryoung, R. A. Inorg. Chem. 1978, 17, 2728.

6. Gale, R.; Osteryoung, R. A. J. Electrochem. Soc., in press.

7. Robinson, J.; Osteryoung, R. A. J. Am. Chem. Soc. 1979, 101, 323.

8. Robinson, J.; Osteryoung, R. A. J. Am. Chem. Soc., in press.

9. Kolthoff, I. M.; Lingane, J. J. "Polarography"; Interscience: New York, 1952; Vol. 1, Chapter 19; Vol. 2, Chapter 40.

10. Baizer, M. M. "Organic Electrochemistry"; Marcel Dekker: New York, 1973; pp. 408-409.

11. Vetter, K. J. "Electrochemical Kinetics"; Academic Press: New York, 1967; pp. 483-487.

12. Peover, M. E. in "Electroanalytical Chemistry", Bard, A. J., Ed.; Marcel Dekker: New York, 1967; Vol. 2, Chapter 1.

13. Jeftic, L.; Manning, G. J. Electroanal. Chem. 1970, 26, 195.

14. Eggins, B. R.; Chambers, J. Q. J. Electrochem. Soc. 1970, 117, 186.

15. Kuder, J. E.; Wychick, D.; Miller, R. L.; Walker, M. S. J. Phys. Chem. 1974, 78 1714.

16. Klopman, G.; Doddapaneni, N. J. Phys. Chem. 1974, 78, 1820, and references cited therein.

17. Masson, J. P.; Devynck, J.; Tremillon, B. J. Electroanal. Chem. 1975, 64, 175, and references cited therein.

18. Brisset, J. L. J. Electroanal. Chem. 1975, 60, 217.

19. Wightman, R. M. Cockrell, J. R.; Murray, R. W.; Burnett, J. N.; Jones, S. B. J. Am. Chem. Soc. 1976, 98, 2562.

20. Bartak, D. E.; Osteryoung, R. A. J. Electroanal. Soc. 1976, 74, 68-83.

21. Robinson, J.; Osteryoung, R. A. J. Electrochem. Soc. 1978, 125, 1454.

22. Grandmougin, E. Chem. Ber. 1906, 39, 3563.

23. Gale, R.; Osteryoung, R. A. Inorg. Chem., in press.

24. Giallonardo, R.; Susz, B. P. Helv. Chim. Acta 1971, 54, 2402.

25. Greig, C. C.; Johnson, C. D. J. Am. Chem. Soc. 1968, 90, 6453.

26. Nepras, M.; Titz, M.; Snobl, D.; Kratochvil, V. Collect. Czechoslovak. Chem. Commun. 1973, 38, 2397.

27. Wawzonek, S.; Berkey, R.; Blaha, E. W.; Runner, M. E. J. Electrochem. Soc. 1956, 103, 456.

28. Robinson, J.; Gilbert, B.; Osteryoung, R. A. Inorg. Chem. 1977, 16, 3040.

29. Peover, M. E.; Davies, J. D. J. Electroanal. Chem. 1963, 6, 46.

30. Barker, G. C.; Bolzan, J. A. Z. Anal. Chem. 1966, 216, 215.

31. Flanagan, J. B.; Takahashi, K.; Anson, F. C. J. Electroanal. Chem. 1977, 85, 257.

32. Oldham, K. B.; Parry, E. P. Anal. Chem. 1966, 38, 867.

33. "CRC Handbook of Cehmistry and Physics", 52nd ed., R. C. Weast, Ed.; The Chemical Rubber Co.; Cleveland, Ohio, 1971 p. F-36.

34. Wawzonek, S. Talanta 1965, 12, 1229.

35. Kalinowski, M. K.; Tenderende-Guminska, B. J. Electroanal. Chem. 1974, 55, 277.

36. Hoijtink, G. I.; von Schooten, J.; de Boer, E.; Aalbersberg, W.I.J. Rec. Trav. Chem., Pays Bas 1954, 73, 355.

37. Mastragostino, M.; Nadjo, L.; Saveant, J. M. Electrochim. Acta 1968, 13, 721.

38. Murray, R. W. In "Techniques of Chemistry", Weissberger, A., Ed.; Wiley-Interscience: New York, 1971; Vol. I, Part IIA, Chapter VIII, pp. 608-611.

39. Nadjo, L.; Saveant, J. M. J. Electroanal. Chem. 1971, 33, 419.

40. Hale, J. M.; Parsons, R. Trans. Faraday Soc. 1963, 59, 1429.

41. Ref. 38, pp. 603-605.

42. Brown, E. R.; Large, R. F. in "Techniques of Chemistry", Weissberger, A., Ed., Wiley-Interscience: New York, 1971; Vol I, Part IIA, Chapter VI, pp. 435-445.

43. Feldberg, S. J. Phys. Chem. 1969, 73, 1238.

44. Jacq, J. Electrochim. Acta 1967, 12, 1345.

45. Albery, W. J.; Hitchman, M. L. "Ring-Disc Electrodes"; Oxford University Press: London, 1971; pp. 38-72.

Table I

Data for titration of AQ with 1.06:1.00 $AlCl_3$:BuPyCl titrant (0.219 M in $Al_2Cl_7^-$). Initial volume = 13.71 ml; initial [AQ] = 3.26 mM. Concentrations of species calculated as follows:

$$[AQ \cdot AlCl_3] = \frac{\text{total mmoles AQ} - [AQ] \cdot V_T}{V_T} \; ; \; (V_T = \text{total volume})$$

$$[Al_2Cl_7^-] = \left[\frac{(0.219)(V_{titrant})}{V_T}\right] - [AQ \cdot AlCl_3]$$

Second break:

$$[AQ \cdot 2AlCl_3] = \frac{\text{total mmoles AQ} - [AQ \cdot AlCl_3] \cdot V_T}{V_T}$$

$$[Al_2Cl_7^-] = \left[\frac{(0.219)(V_{titrant})}{V_T}\right] - 2[AQ \cdot 2AlCl_3] - [AQ \cdot AlCl_3]$$

First Break

$V_{titrant}$, µl (cumulative total)	$i_{NPV,\mu A}/C^a$, mM [AQ]	$[AQ \cdot AlCl_3]$ mM	$[Al_2Cl_7^-]$ mM	K_1
0	220/3.26	0	-	-
50	200/2.96	0.29	0.51	778
100	179/2.65	0.59	1.00	902
192	156/2.31	0.91	2.12	753
278	139/2.06	1.13	3.22	690

Mean (Std. Dev.) 781 (89)

Second Break

	$i_{NPV,\mu A}/C^b$, mM $[AQ \cdot AlCl_3]$	$[AQ \cdot 2AlCl_3]$ mM	$[Al_2Cl_7^-]$ mM	K_2
719	112/2.10	1.00	6.81	283
799	108/2.02	1.06	7.92	266
1,039	90/1.69	1.34	11.06	290
1,234	72/1.35	1.64	13.46	366

Mean (Std. Dev.) 301 (44)

[a] Based on D value for AQ in neutral melt of 1.4×10^{-6} cm^2/sec.

[b] Based on D value for $AQ \cdot AlCl_3$ of 8.4×10^{-7} cm^2/sec, calculated from data in first break.

FIGURE CAPTIONS

1. Cyclic voltammograms of 9,10-anthraquinone (AQ) in 0.8:1.0 basic melt (top scan); in neutral melt, acidity adjusted by small additions of $AlCl_3$ (middle three scans); in 1:2:1.0 acidic melt (bottom scan). Scans recorded at 40°C, 200mV/sec scan rate, AQ concentration 4.0mM.

2. Infrared spectra of AQ in melts of various acidities.

   (a) 0.8:1.0 Basic melt; [AQ] = 34mM.

   (b) Neutral melt; $[AQ \cdot AlCl_3]$ = 32mM; $[AQ \cdot 2AlCl_3]$ = 17mM.

   (c) 1.2:1.0 Acidic melt; $[AQ \cdot 2AlCl_3]$ = 14mM.

   Arrows indicate bands due to AQ species; other bands are due to n-butyl pyridinium cation. Concentrations were estimated by normal pulse voltammetry prior to infrared spectroscopic analysis.

3. Nernst plot obtained by coulometrically varying $[AQ]/[AQ^{=}]$ ratio. Melt composition: 0.8:1.0 Basic melt. Total [AQ] = 2.8mM.

4. Nernst plot obtained by varying basic melt composition with addition of BuPyCl. $[AQ] = [AQ^{=}]$ = 3.6mM, by initial coulometric reduction of AQ-containing melt.

5. Normal pulse voltammograms of AQ in 0.8:1.0 basic melt. [AQ] = 3.3mM. Pulse width = 48 msec; scan rate = 5mV/sec; interval between pulses = 0.5 second.

   (a) Initial potential = -0.20 V; cathodic scan.

   (b) Initial potential = -0.80 V; anodic scan (reverse pulse voltammetry).

6. Plot of log ($i/\mu A$) vs. log (τ/msec) for normal pulse voltammetric data in neutral melt containing total AQ concentration of 9.8mM; distribution of species is similar to that shown in Figure 1, second scan. τ values refer to times corresponding to the middle of the sampling interval (75-99% of pulse width). Scan rate = 5mV/sec; interval between pulses = 10 x pulse width.

7. Diagram illustrating electrochemical reaction pathways for AQ reduction in the melt. Horizontal paths represent electron transfers, while vertical paths represent interactions of AQ species with melt constituents.

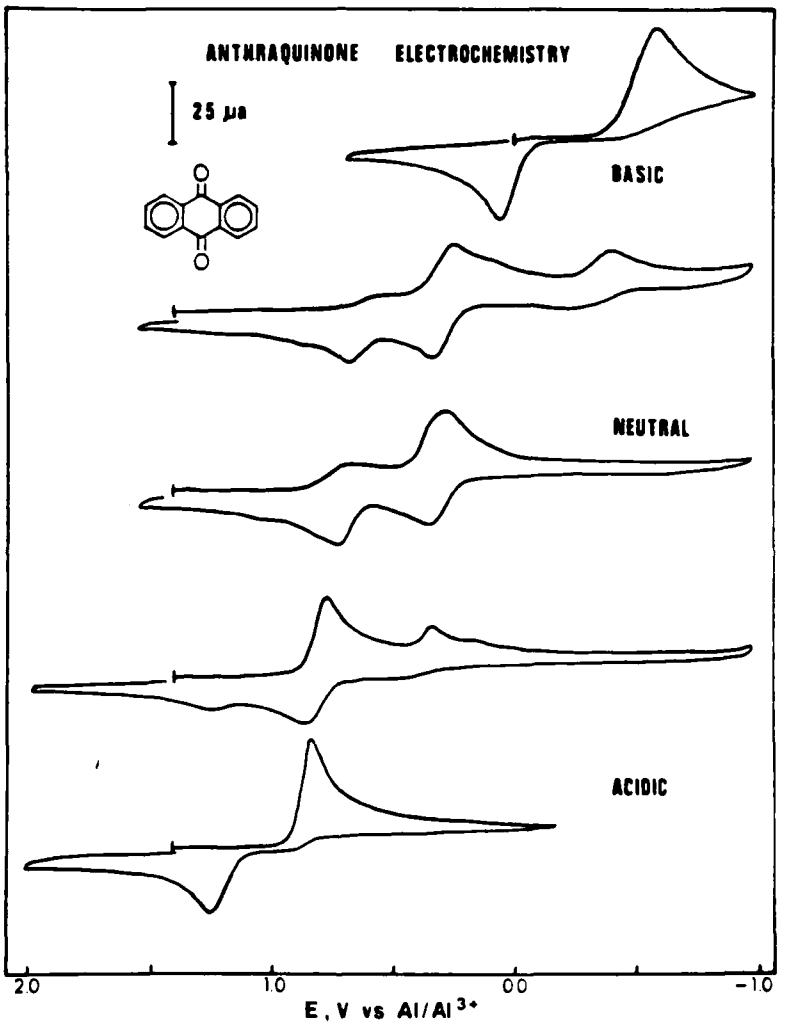
ANTHRAQUINONE ELECTROCHEMISTRY
25 μa
BASIC
NEUTRAL
ACIDIC
2.0
1.0
0.0
-1.0
E, V vs Al/Al 3+

Figure 1

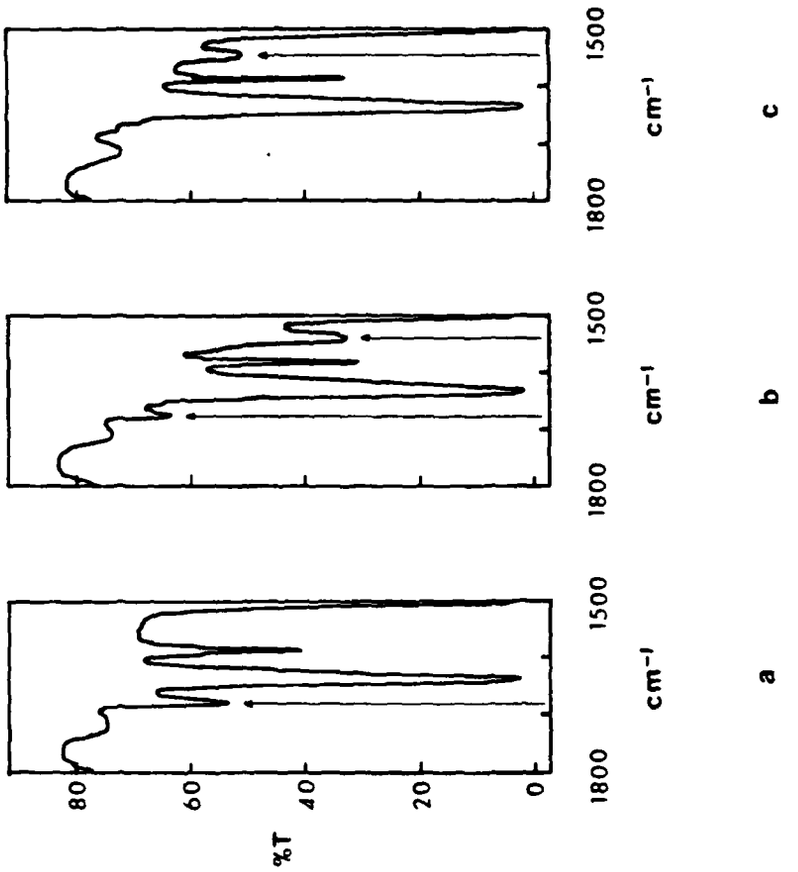

Figure 2

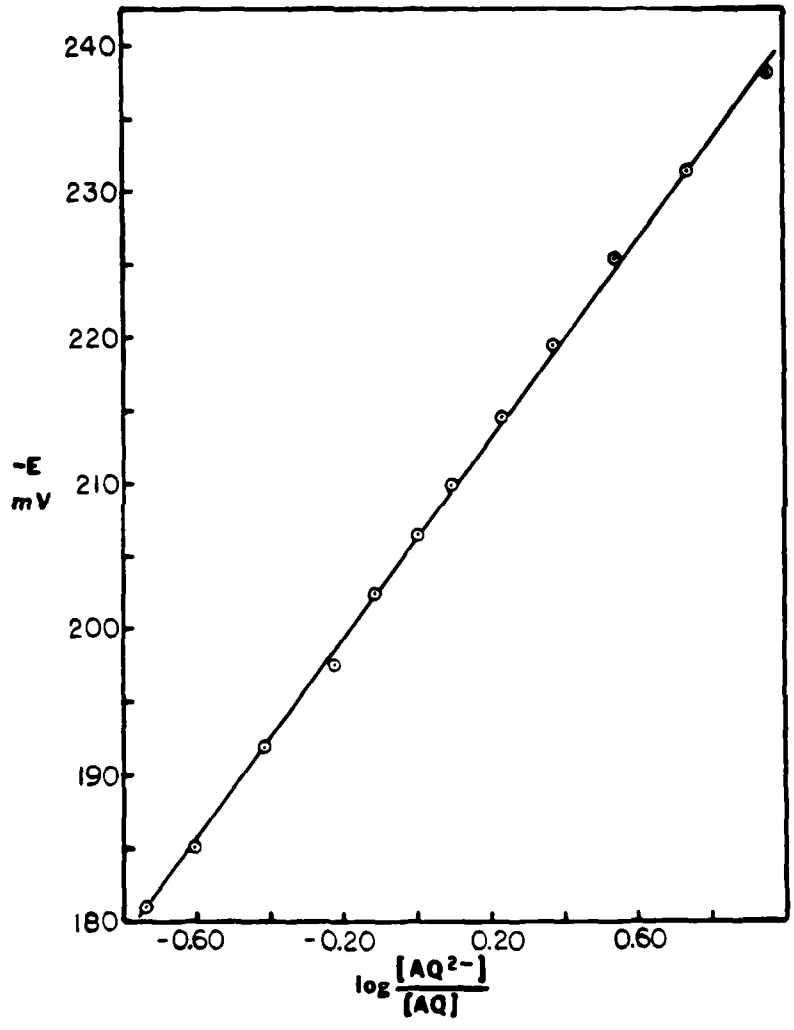

Figure 3

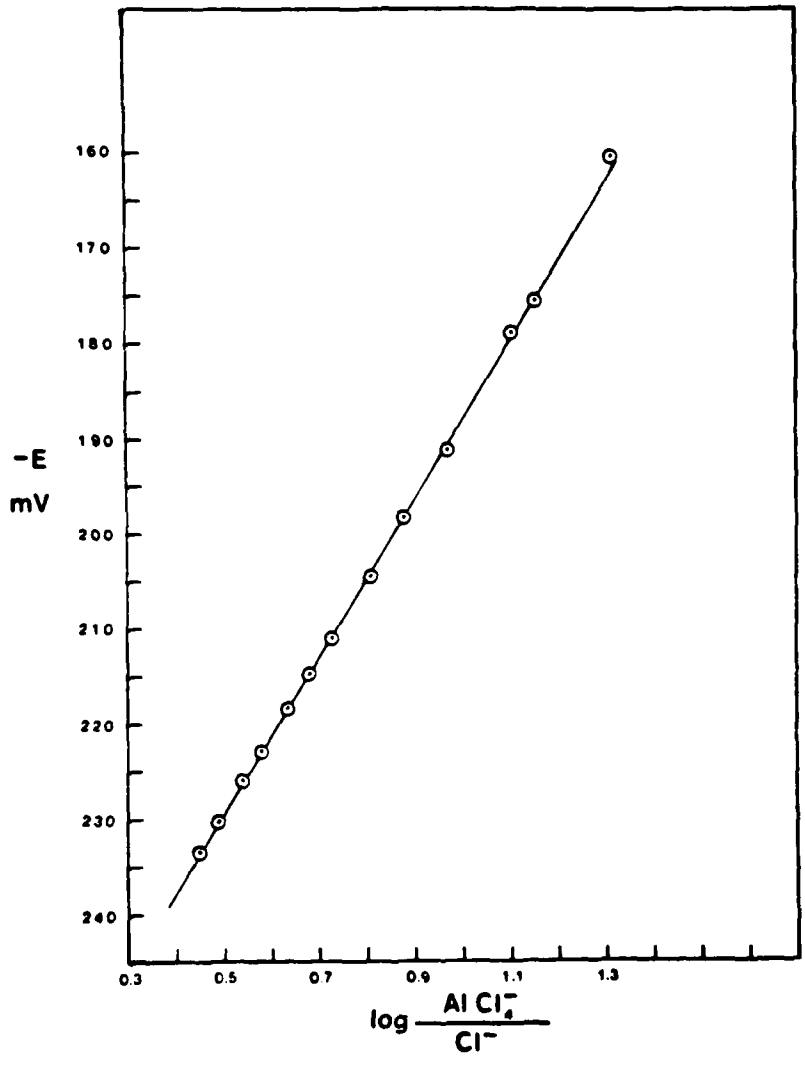
160
170
180
190
200
210
220
230
240
-E
mV
0.3
0.5
0.7
0.9
1.1
1.3
log Al Cl4- / Cl-

Figure 4

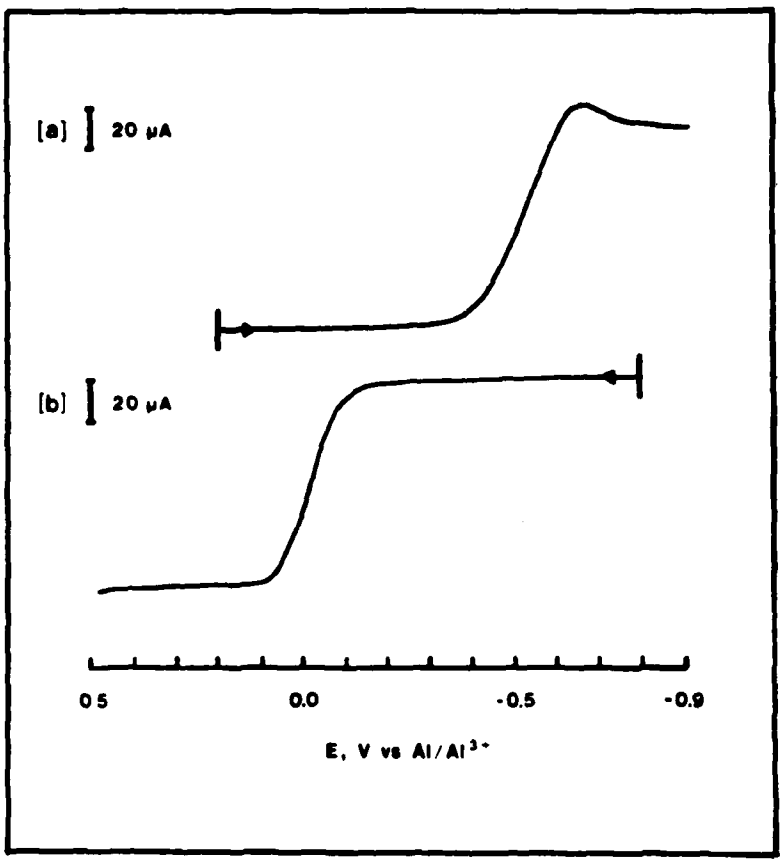

Figure 5

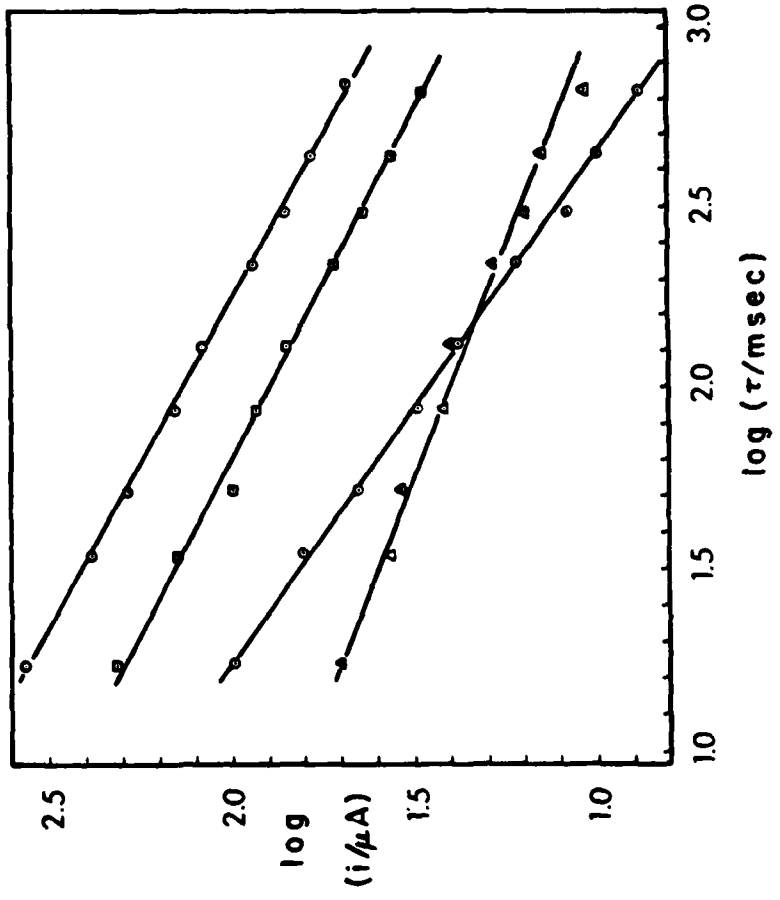

Figure 6

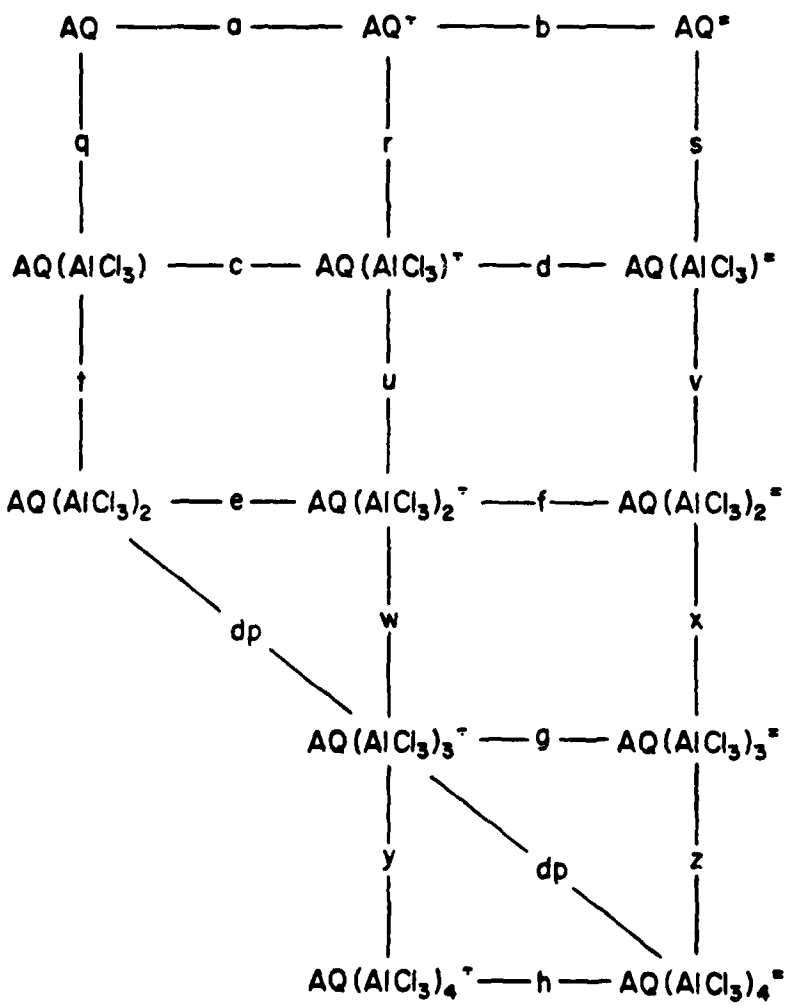
AQ
a
AQ⁻
b
AQ⁼
q
r
s
AQ(AlCl3)
c
AQ(AlCl3)⁻
d
AQ(AlCl3)⁼
t
u
v
AQ(AlCl3)2
e
AQ(AlCl3)2⁻
f
AQ(AlCl3)2⁼
dp
w
x
AQ(AlCl3)3⁻
g
AQ(AlCl3)3⁼
y
dp
z
AQ(AlCl3)4⁻
h
AQ(AlCl3)4⁼

Figure 7

472:GAN:716:tam
78u472-608

TECHNICAL REPORT DISTRIBUTION LIST, GEN

	No. Copies
Dr. M. B. Denton University of Arizona Department of Chemistry Tucson, Arizona 85721	1
Dr. B. R. Kowalski University of Washington Department of Chemistry Seattle, Washington 98105	1
Dr. D. L. Venezky Naval Research Laboratory Code 6130 Washington, D.C. 20375	1
Dr. H. Freiser University of Arizona Department of Chemistry Tuscon, Arizona 85721	1
Dr. Fred Saalfeld Naval Research Laboratory Code 6110 Washington, D.C. 20375	1
Dr. H. Chernoff Massachusetts Institute of Technology Department of Mathematics Cambridge, Massachusetts 02139	1
Dr. K. Wilson University of California, San Diego Department of Chemistry La Jolla, California	1
Dr. A. Zirino Naval Undersea Center San Diego, California 92132	1

472:GAN:716:tam
78u472-608

TECHNICAL REPORT DISTRIBUTION LIST,

	No. Copies
Dr. John Duffin United States Naval Postgraduate School Monterey, California 93940	1
Dr. G. M. Hieftje Department of Chemistry Indiana University Bloomington, Indiana 47401	1
Dr. Victor L. Rehn Naval Weapons Center Code 3813 China Lake, California 93555	1
Dr. Christie G. Enke Michigan State University Department of Chemistry East Lansing, Michigan 48824	1
Dr. Kent Eisentraut, MBT Air Force Materials Laboratory Wright-Patterson AFB, Ohio 45433	1
Walter G. Cox, Code 3632 Naval Underwater Systems Center Building 148 Newport, Rhode Island 02840	1
Office of Naval Research 800 North Quincy Street Arlington, Virginia 22217 Attn: Code 472	1 2
ONR Branch Office 536 S. Clark Street Chicago, Illinois 60605 Attn: Dr. George Sandoz	1

472:GAN:716:tam
78u472-608

TECHNICAL REPORT DISTRIBUTION LIST,

	No. Copies
ONR Branch Office 715 Broadway New York, New York 10003 Attn: Scientific Dept.	1
ONR Branch Office 1030 East Green Street Pasadena, California 91106 Attn: Dr. R. J. Marcus	1
ONR Area Office One Hallidie Plaza, Suite 601 San Francisco, California 94102 Attn: Dr. P. A. Miller	1
ONR Branch Office Building 114, Section D 666 Summer Street Boston, Massachusetts 02210 Attn: Dr. L. H. Peebles	1
Director, Naval Research Laboratory Washington, D.C. 20390 Attn: Code 6100	1
The Assistant Secretary of the Navy (R,E&S) Department of the Navy Room 4E736, Pentagon Washington, D.C. 20350	1
Commander, Naval Air Systems Command Department of the Navy Washington, D.C. 20360 Attn: Code 310C (H. Rosenwasser)	1
Defense Documentation Center Building 5, Cameron Station Alexandria, Virginia 22314	12

472:GAN:716:tam
78u472-608

TECHNICAL REPORT DISTRIBUTION LIST,

	No. of Copies
U.S. Army Research Office P.O. Box 1211 Research Triangle Park, N.C. 27709 Attn: CRD-AA-IP	1
Naval Ocean Systems Center San Diego, California 92152 Attn: Mr. Joe McCartney	1
Naval Weapons Center China Lake, California 93555 Attn: Dr. A. B. Amster Chemistry Division	1
Naval Civil Engineering Laboratory Port Hueneme, California 93401 Attn: Dr. R. W. Drisko	1
Professor K. E. Woehler Department of Physics & Chemistry Naval Postgraduate School Monterey, California 93940	1
Dr. A. L. Slafkosky Scientific Advisor Commandant of the Marine Corps (Code RD-1) Washington, D.C. 20380	1
Office of Naval Research 800 N. Quincy Street Arlington, Virginia 22217 Attn: Dr. Richard S. Miller	1
Naval Ship Research and Development Center Annapolis, Maryland 21401 Attn: Dr. G. Bosmajian Applied Chemistry Division	1
Naval Ocean Systems Center San Diego, California 91232 Attn: Dr. S. Yamamoto, Marine Sciences Division	1

472:GAN:716:tam
78u472-608

TECHNICAL REPORT DISTRIBUTION LIST,

	No. Copies
Dr. Paul Delahay New York University Department of Chemistry New York, New York 10003	1
Dr. E. Yeager Case Western Reserve University Department of Chemistry Cleveland, Ohio 41106	1
Dr. D. N. Bennion University of California Chemical Engineering Department Los Angeles, California 90024	1
Dr. R. A. Marcus California Institute of Technology Department of Chemistry Pasadena, California 91125	1
Dr. J. J. Auborn Bell Laboratories Murray Hill, New Jersey 07974	1
Dr. Adam Heller Bell Telephone Laboratories Murrary Hill, New Jersey 07974	1
Dr. T. Katan Lockheed Missiles & Space Co, Inc. P.O. Box 504 Sunnyvale, California 94088	1
Dr. Joseph Singer, Code 302-1 NASA-Lewis 21000 Brookpark Road Cleveland, Ohio 44135	1
Dr. B. Brummer EIC Incorporated Five Lee Street Cambridge, Massachusetts 02139	1

472:GAN:716:tam
78u472-608

TECHNICAL REPORT DISTRIBUTION LIST, 359

	No. Copies
Library P. R. Mallory and Company, Inc. Northwest Industrial Park Burlington, Massachusetts 01803	1
Dr. P. J. Hendra University of Southhampton Department of Chemistry Southhampton SO9 5NH United Kingdom	1
Dr. Sam Perone Purdue University Department of Chemistry West Lafayette, Indiana 47907	1
Dr. Royce W. Murray University of North Carolina Department of Chemistry Chapel Hill, North Carolina 27514	1
Naval Ocean Systems Center San Diego, California 92152 Attn: Technical Library	1
Dr. J. H. Ambrus The Electrochemistry Branch Materials Division, Research & Technology Department Naval Surface Weapons Center White Oak Laboratory Silver Spring, Maryland 20910	1
Dr. G. Goodman Globe-Union Incorporated 5757 North Green Bay Avenue Milwaukee, Wisconsin 53201	1
Dr. J. Boechler Electrochimica Corporation Attention: Technical Library 2485 Charleston Road Mountain View, California 94040	1

472:GAN:716:tam
78u472-608

TECHNICAL REPORT DISTRIBUTION LIST, 359

	No. Copies
Dr. P. P. Schmidt Oakland University Department of Chemistry Rochester, Michigan 48063	1
Dr. H. Richtol Chemistry Department Rensselaer Polytechnic Institute Troy, New York 12181	1
Dr. A. B. Ellis Chemistry Department University of Wisconsin Madison, Wisconsin 53706	1
Dr. M. Wrighton Chemistry Department Massachusetts Institute of Technology Cambridge, Massachusetts 02139	1
Larry E. Plew Naval Weapons Support Center Code 3073, Building 2906 Crane, Indiana 47522	1
S. Ruby DOE (STOR) 600 E Street Washington, D.C. 20545	1
Dr. Aaron Wold Brown University Department of Chemistry Providence, Rhode Island 02192	1
Dr. R. C. Chudacek McGraw-Edison Company Edison Battery Division Post Office Box 28 Bloomfield, New Jersey 07003	1
Dr. A. J. Bard University of Texas Department of Chemistry Austin, Texas 78712	1

472:GAN:716:tam
78u472-608

TECHNICAL REPORT DISTRIBUTION LIST, 359

	No. of Copies
Dr. M. M. Nicholson Electronics Research Center Rockwell International 3370 Miraloma Avenue Anaheim, California 92803	1
Dr. M. G. Sceats University of Rochester Department of Chemistry Rochester, New York 14627	1

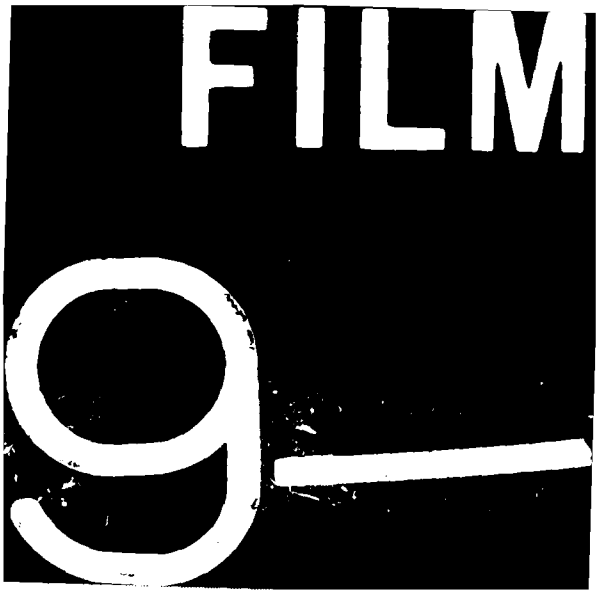
FILM
9